processes

MDPI

Article

Phase-Field Modeling of Hydraulic Fracture in Porous Media with In Situ Stresses

Tao You [1,2,3]

[1] Key Laboratory of Ministry of Education for Geomechanics and Embankment Engineering, Hohai University, Nanjing 210098, China; tao.you@unileoben.ac.at
[2] College of Civil and Transportation Engineering, Hohai University, Nanjing 210098, China
[3] Department Geoenergy, Montanuniversität Leoben, 8700 Leoben, Austria

Abstract: While the variational phase-field model has been widely used in modeling fracturing in porous media, it poses a challenge when applying high confining pressures on a model because the relatively large deformation induced by the confining pressures might cause undesired crack nucleation when the strain decomposition scheme are used, which is not consistent with engineering observations. This study proposes a two-step strategy to incorporate in situ stresses into phase-field modeling of hydraulic fractures, addressing the limitations of previous approaches in capturing realistic fracture initiation and propagation under high confinement. A micromechanics-based hydromechanical phase-field model is presented first, and the proposed two-step strategy is investigated with different strain decomposition schemes: isotropic, volumetric–deviatoric, and no-tension models. Two numerical examples show that the two-step strategy effectively achieves a desired initial state with geostatic stresses and zero strain, allowing for accurate simulations even in the presence of complex natural fractures. The efficiency of the proposed two-step strategy for incorporating in situ stresses is highlighted, and the challenges associated with capturing stiffness recovery and shear fracture nucleation under high confinement using strain-based models are discussed.

Keywords: phase-field method; hydraulic fracture; in situ stress; natural fractures; crack growth

check for updates

Citation: You, T. Phase-Field Modeling of Hydraulic Fracture in Porous Media with In Situ Stresses. *Processes* **2024**, *12*, 1671. https://doi.org/10.3390/pr12081671

Academic Editor: Zheng Sun

Received: 15 July 2024
Revised: 31 July 2024
Accepted: 8 August 2024
Published: 9 August 2024

Copyright: © 2024 by the authors. Licensee MDPI, Basel, Switzerland. This article is an open access article distributed under the terms and conditions of the Creative Commons Attribution (CC BY) license (https://creativecommons.org/licenses/by/4.0/).

1. Introduction

As part of the ongoing energy transition process, facilitating or inhibiting the fracturing of rocks is becoming increasingly important, as they play a key role in exploiting energy sources such as oil, natural gas, and geothermal heat [1], or in the assessment of effective energy storage [2] and CO_2 sequestration [3] repositories. Fluid-driven (hydraulic) fracturing, which induces fractures by injecting fluids into rock formations, plays a pivotal role in this regard. This process, while successful in unlocking vast reserves of hydrocarbons, presents significant challenges in terms of predicting and controlling fracture network development. Traditional approaches like discrete fracture network (DFN) models, which explicitly represent fractures as discrete elements within the rock, often struggle to capture the complex interplay between fracture growth, fluid flow, and the surrounding porous medium, especially when dealing with highly heterogeneous and complex reservoir formations. These models also face limitations in representing the evolution of fracture networks, requiring computationally expensive re-meshing processes as fractures propagate [4,5].

The phase-field method offers an elegant and computationally efficient solution for simulating fracture propagation in porous media. This method, pioneered by Bourdin et al. [6], utilizes a scalar field variable, known as the phase-field, to represent the fracture. This field smoothly transitions from zero (unfractured material) to one (completely fractured material), allowing for seamless representation of complex fracture geometries and avoiding the need for mesh re-meshing. This approach has been successfully applied to simulate various fracture phenomena, including crack propagation in brittle materials [7,8], dynamic fracture [9], and hydraulic fracture [10–13]. For hydraulic fracturing in porous media,

the phase-field model naturally couples the fracture mechanics with the fluid flow within the porous medium, offering a more realistic and comprehensive representation of the fracture network evolution. Furthermore, the interaction of hydraulic fractures with natural fractures has been handily addressed, for example, in [14–17].

However, accurately predicting the behavior of hydraulic fractures in porous media requires careful consideration of in situ stresses arising from tectonic forces, overburden pressure, and pore fluid pressure, which will influence fracture initiation, propagation direction, and the overall fracture network development [18,19]. The classic Hubbert and Willis approach [20] has shown that the critical pressure required to initiate these fractures (known as the breakdown pressure) is determined by the geostatic stresses in the rock as well as the mechanical strength of the rock. Neglecting these stresses can lead to inaccurate predictions of fracture geometry and fluid flow patterns, ultimately affecting the effectiveness of hydraulic fracturing operations. Incorporating in situ stresses into the phase-field model demands capturing the complex interactions between the injected fluid pressure, the surrounding porous medium, and the preexisting stresses within the rock. Several approaches have been proposed to incorporate in situ stress into the phase-field model. Zhou et al. [21] modified the energy functional for the phase-field model [21] to include the contribution of the initial stresses. Nevertheless, the validation of this approach for different strain decomposition schemes is not ensured. Enrico Salvati [22] introduced a hydrostatic eigenstrain field into the phase-field model to consider initial stresses. The eigenstrain approach is self-consistent, satisfying both stress balance and strain compatibility, but the method is relatively complex, involves the computation of R-curves, and is not conducive to engineering applications, as argued by [23]. Zhang et al. [23] further introduced an initial equilibrium iteration to obtain the initial stress value and phase field value. However, this approach is based on the stress-based fracture criterion, and its extension to the strain-based fracture criterion is questionable.

This paper aims to present a general approach to incorporating in situ stresses into the phase-field modeling of hydraulic fractures. The proposed method is based on the concept of eigenstrain used by [22] but, different from existing work, will employ two-step numerical computation to achieve realistic initial stresses and pressure states for various strain decomposition schemes. We will first delve into the theoretical formulation of the variational phase-field approach in the modeling of hydraulic fracturing and then propose a two-step strategy to calculate the eigenstrain caused by the in situ stresses. Therefore, high confining pressures can be applied freely without inducing undesired crack evolution at the beginning of the simulation. Using two numerical examples, i.e., hydraulic fracture nucleation from a borehole and interaction with pre-existing natural fractures, various strain decomposition schemes are investigated, highlighting the validity of the proposed two-step strategy. Furthermore, the advantages and limitations of different strain decomposition schemes are presented.

2. Methods

2.1. Model Formulations

2.1.1. Energy Functional

The phase-field method will be used in the simulation of hydraulic fracturing in a porous solid Ω subjected to displacement $\bar{\boldsymbol{u}}$ on the boundary $\partial\Omega_u$. You and Yoshioka [24] compared existing hydromechanical phase-field models and proposed a micromechanics-based formulation, which will be used in this paper. Following this, the poroelastic strain energy is defined as a function of displacement $\boldsymbol{u}$, phase-field v, and pressure p, i.e.,

$$W(\boldsymbol{u}, v, p) = \int_{\Omega} \psi(\boldsymbol{u}, v)\, \mathrm{d}V + \int_{\Omega} \frac{p^2}{2M(v)}\, \mathrm{d}V, \tag{1}$$

where Ω denotes the research body, $M(v)$ is Biot's modulus related to the phase-field variable, and ψ denotes the strain energy per unit volume and has the following general form:

$$\psi(\boldsymbol{u}, v) = g(v)\psi_+(\boldsymbol{u}) + \psi_-(\boldsymbol{u}), \tag{2}$$

with $g(v)$ being the degradation function, which will be taken as $g(v) = v^2$ in this paper.

For the isotropic model, we have

$$\psi_+(\boldsymbol{u}) = \frac{1}{2}\boldsymbol{\varepsilon} : \mathbb{C} : \boldsymbol{\varepsilon},\ \psi_-(\boldsymbol{u}) = 0, \tag{3}$$

where $\boldsymbol{\varepsilon}$ denotes the elastic strain, and $\mathbb{C}$ is the stiffness tensor.

For the volumetric–deviatoric decomposition model [25], we have

$$\psi_+(\boldsymbol{u}) = \frac{k}{2}\langle \mathrm{Tr}[\boldsymbol{\varepsilon}]\rangle_+^2 + \mu\boldsymbol{\varepsilon} : \mathbb{K} : \boldsymbol{\varepsilon},\ \psi_-(\boldsymbol{u}) = \frac{k}{2}\langle \mathrm{Tr}[\boldsymbol{\varepsilon}]\rangle_-^2, \tag{4}$$

where k is the bulk modulus, $\mathrm{Tr}[\cdot]$ is the trance operator, and $\langle\rangle_+ = (\cdot + |\cdot|)/2$ and $\langle\rangle_- = (\cdot - |\cdot|)/2$ are the Macaulay brackets.

For the masonry-like model [26], also called the no-tension model, we have

$$\psi_+(\boldsymbol{u}) = \frac{\lambda}{2}(\mathrm{Tr}[\boldsymbol{\varepsilon}_+])^2 + \mu\boldsymbol{\varepsilon}_+ : \boldsymbol{\varepsilon}_+,\ \psi_-(\boldsymbol{u}) = \frac{\lambda}{2}(\mathrm{Tr}[\boldsymbol{\varepsilon}_-])^2 + \mu\boldsymbol{\varepsilon}_- : \boldsymbol{\varepsilon}_-, \tag{5}$$

where λ and μ are Lamé constants. The strain is decomposed so that the positive strain $\boldsymbol{\varepsilon}^+$ is a positive definite tensor and is coaxial with $\boldsymbol{\varepsilon}$:

$$\boldsymbol{\varepsilon}_+ = \sum_i \langle \varepsilon_i \rangle_+ \mathbf{n}_i \otimes \mathbf{n}_i$$

and

$$\boldsymbol{\varepsilon}_- = \sum_i (\varepsilon_i - \langle \varepsilon_i \rangle_+) \mathbf{n}_i \otimes \mathbf{n}_i,$$

with ε_i and $\boldsymbol{n}_i$ being the eigenvalue and eigenvector of $\boldsymbol{\varepsilon}$, respectively.

Then, by considering the crack surface energy, the total energy functional for a poroelastic medium can be written as

$$\mathcal{F}_\ell(\boldsymbol{u}, v, p) := W(\boldsymbol{u}, v, p) + \int_\Omega \frac{3G_c}{8}\left[\frac{(1-v)}{\ell} + \ell\nabla v \cdot \nabla v\right] \mathrm{d}V, \tag{6}$$

where the `AT1` phase-field model [27] is used in this paper, while G_c denotes the crack surface energy density, ℓ the length scale parameter, and ∇ the gradient operator.

2.1.2. Fluid Mass Balance Law

The variation of fluid content is defined as

$$\zeta := \phi - \phi_0 = \alpha(v)\nabla \cdot \boldsymbol{u} + \frac{p}{M(v)}, \tag{7}$$

where ϕ denotes the porosity of the porous media, and $\nabla\cdot$ is the divergence operator. Biot's coefficient α and Biot's modulus M are functions of the phase-field variable, which accounts for the alteration of the rock property due to crack growth. The derivation based on micromechanical analysis gives the following definitions [24], i.e.,

$$\alpha(v) = 1 - \frac{k_{\mathrm{eff}}}{k_{\mathrm{m}}}(1 - \alpha_{\mathrm{m}}), \tag{8}$$

$$\frac{1}{M(v)} = \frac{\alpha(v) - \phi}{k_{\mathrm{m}}}(1 - \alpha_{\mathrm{m}}), \tag{9}$$

where k_{eff} is the effective (phase-field degraded) bulk modulus, and its form depends on which phase-field model is used in Equations (3)–(5). Additionally, k_{m} and α_{m} are the bulk modulus and Biot's coefficient of the intact porous medium, respectively.

Considering the slightly compressive fluid, the mass balance equation for the fractured porous media can be written as [24]:

$$\left[\frac{1}{M(v)} + c_{\text{f}}\phi\right]\frac{\partial p}{\partial t} + \alpha(v)\nabla\cdot\frac{\partial \boldsymbol{u}}{\partial t} + \nabla\cdot\frac{\boldsymbol{K}}{\mu_{\text{f}}}(-\nabla p + \rho_{\text{f}}\boldsymbol{g}) = Q, \tag{10}$$

where c_{f} denotes the fluid compressibility, ρ_{f} the fluid density, μ_{f} the fluid viscosity, $\boldsymbol{g}$ the gravitational acceleration, Q the source/sink term, and K the permeability that will be enhanced by crack growth, which is defined as

$$\boldsymbol{K} = K_{\text{m}}\boldsymbol{I} + (1-v)^{\xi}\frac{w^2}{12}(\boldsymbol{I} - \boldsymbol{n}_\Gamma \otimes \boldsymbol{n}_\Gamma), \tag{11}$$

with K_m being the permeability of the porous media, ξ a constant [10] taken as 10 in this paper, ω the fracture width, and $\boldsymbol{n}_\Gamma$ the normal direction of fracture. In this paper, both ω and $\boldsymbol{n}_\Gamma$ are estimated locally by

$$\begin{cases} w = h_e\varepsilon_1 \\ \boldsymbol{n}_\Gamma = \mathbf{n}_1 \end{cases}, \tag{12}$$

where h_e is the minimum element size. Note that Equation (12) leads to accurate estimation of $\boldsymbol{n}_\Gamma$ and w for a toughness-dominated hydraulic fracture [28], i.e., low viscous fluid, which is the assumption in this paper. When the fluid viscosity is high, the pressure gradient along the fracture path is sufficient to cause the main strain direction to coincide with the fracture path but not the normal direction. In this case, a delicate method may be required, for example, level-set [29] or image processing [30].

2.1.3. Governing Equations

The governing equations of displacement and phase-field can be derived using alternate minimization to the energy functional (6) in admissible spaces. Therefore, we can write

$$(\boldsymbol{u}, v) = \underset{\boldsymbol{u},v}{\operatorname{argmin}}\{\mathcal{F}_\ell(\boldsymbol{u}, v) : \mathbf{u} \in \mathcal{U}, v \in \mathcal{V}(t_i)\}, \tag{13}$$

where $\mathcal{U}$ is the kinematically admissible displacement set

$$\mathcal{U} = \left\{\boldsymbol{u} \in H^1(\Omega) : \boldsymbol{u} = \bar{\boldsymbol{u}} \quad \text{on} \quad \partial\Omega_u\right\}, \tag{14}$$

and the admissible set of v is

$$\mathcal{V}(t_i) = \left\{v \in H^1(\Omega) : 0 \le v(x,t_i) \le v(x,t_{i-1}) \le 1 \ \forall x \text{ s.t. } v(x,t_{i-1}) \le v_{\text{irr}}\right\}, \tag{15}$$

where v_{irr} is a threshold value less than which the crack's irreversibility is ensured.

Combining Equations (6) and (13), we have

$$\nabla\cdot\boldsymbol{\sigma} = \mathbf{0}, \tag{16}$$

$$g'(v)\left[\psi^+ + \frac{p^2(1-\alpha_{\text{m}})^2}{2k_{\text{m}}}\right] + \frac{3G_{\text{c}}}{8}\left(\frac{-1}{\ell} + 2\ell\nabla\cdot\nabla v\right) = 0, \tag{17}$$

where $\boldsymbol{\sigma}$ is the total stress, which is defined as

$$\boldsymbol{\sigma} = \frac{\partial W}{\partial \boldsymbol{\varepsilon}} = \mathbb{C}_{\text{eff}} : \boldsymbol{\varepsilon} - \alpha p\boldsymbol{I}, \tag{18}$$

where $\mathbb{C}_{\text{eff}}$ is the effective stiffness tensor, whose expression depends on the used strain decomposition method. For example, the isotropic model gives $\mathbb{C}_{\text{eff}} = g(v)\mathbb{C}$.

This hydraulic fracture phase-field model has been implemented in the open-source software OpenGeoSys (https://www.opengeosys.org/) [31]. The solution for the three-field problem follows a staggered scheme, in which we first solve the phase-field v and then iteratively solve pressure p and displacement $\boldsymbol{u}$. After convergence on the $u - p$ iteration, we repeat this until all three fields are converged. The fixed stress split is used to solve the hydromechanical coupling problem [32].

2.2. Initial State

The formations may have undergone prolonged tectonic processes, leading to complex geostatic stresses also affected by local geological structures and heterogeneity. The full history of geological tectonics is untraceable, and the same is the case for local strain. Therefore, the initial state is commonly considered zero strain with initial geostatic stresses. When initial stress $\boldsymbol{\sigma}_0$ and initial pore pressure p_0 are considered, the total stress becomes

$$\boldsymbol{\sigma} - \boldsymbol{\sigma}_0 = \mathbb{C}_{\text{eff}} : \boldsymbol{\varepsilon} - \alpha(p - p_0)\boldsymbol{I}. \tag{19}$$

However, for the phase-field model, the most widely used models are strain-based, which means the geostatic stress has to be reproduced by strain ε_{r}. In this paper, we call strain $\boldsymbol{\varepsilon}^*$ an eigenstrain, which will be relieved with crack growth. Given this, we can rewrite Equation (19) into

$$\boldsymbol{\sigma} = \mathbb{C}_{\text{eff}} : \boldsymbol{\varepsilon} + \boldsymbol{\sigma}_0 - \alpha(p - p_0)\boldsymbol{I} = \mathbb{C}'_{\text{eff}} : (\boldsymbol{\varepsilon} + \boldsymbol{\varepsilon}^*) - \alpha(p - p_0)\boldsymbol{I}, \tag{20}$$

where $\mathbb{C}'_{\text{eff}}$ is related to the total strain $\boldsymbol{\varepsilon} + \boldsymbol{\varepsilon}^*$.

Apparently, the transition from $\boldsymbol{\sigma}_0$ to $\boldsymbol{\varepsilon}^*$ depends on the specific energy split strategy, for example, Equations (3)–(5), and also the geometry and boundary conditions of the model. In particular, the pre-existing natural fractures or heterogeneity will disrupt local geostatic stress, making the theoretical calculation on $\boldsymbol{\varepsilon}^*$ impossible, as previously done in [22].

In this paper, we propose the following two steps to achieve this initial state without triggering undesired phase-field evolution when applying confining pressure to numerical models and accommodating any energy split methods.

- Step 1: Apply confining pressure and boundary conditions to the model and provide a large enough value of G_{c} and long-term time to calculate the displacement and pressure fields.

In this step, we assign a high G_{c} to avoid an undesired phase-field evolution when high confining pressure is applied. A long-term time is to ensure the pore pressure can be fully dispersed. Certainly, the pore pressure might not disperse completely, and in this case, a realistic consolidation time can be used. In this paper, we assume the pore pressure is fully dispersed after many years of consolidation. As such, we obtain the displacement $\boldsymbol{u}_0$ and p_0.

- Step 2: Input the resulting $\boldsymbol{u}_0$ and p_0 as initial displacement and pressure fields and apply the real G_{c} for the simulation.

In this step, the initial displacement $\boldsymbol{u}_0$ is used to calculate the eigenstrain $\boldsymbol{\varepsilon}^*$. As mentioned above, this eigenstrain is equivalent to applying an initial stress $\boldsymbol{\sigma}_0$, which can reach equilibrium with external loading. Therefore, the real strain $\boldsymbol{\varepsilon}$ remains zero, which will not lead to crack growth.

As a result, this two-step strategy is compatible with various energy split methods and will not generate fictitious crack growth when considering geostatic stress for naturally fractured media.

3. Results and Discussions

In this section, two numerical examples are established to verify the validity of the proposed two-step method, where the first numerical example investigates the crack nucleation from a borehole caused by fluid pressurization, and the second shows the interaction between the hydraulic fracture with the natural fractures. Both numerical examples are under the plane strain condition.

3.1. In Situ Stresses for Different Strain Decomposition Schemes

We first verified the proposed method for applying in situ stresses to a homogeneous model and a model with randomly distributed natural fractures. Three commonly used strain decomposition schemes, i.e., the isotropic model, the volumetric–deviatoric model by [25], and the no-tension model by [26] (the material does not support tension), were considered. The geometry of the homogeneous model is illustrated in Figure 1a, where a borehole is located in the center of the model with a diameter of 0.1 m. Each midpoint of the edge is supported by a roll. Vertical confining pressure σ_v was applied to the top and bottom edges, and horizontal pressure σ_v was applied to the left and right edges.

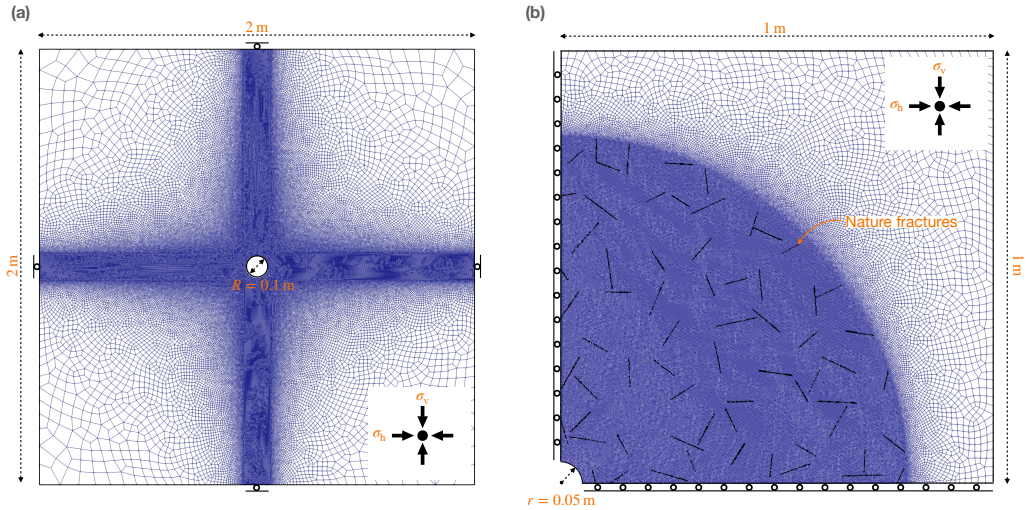


Figure 1. The geometry, mesh, and boundary conditions of the numerical models, where (**a**) is used for nucleation and propagation of the hydraulic fracture from a borehole, and (**b**) is used to investigate the interaction between the hydraulic fracture and natural fractures.

Figure 1b shows the naturally fractured model, which is one-quarter of the homogeneous model. The natural fractures were randomly generated with lengths ranging from 0.02 m to 0.1 m. The phase field in the fracture domain was set to 0 (fully broken).

Vertical and horizontal confining pressures were set to 9.7 MPa and 17.2 MPa, respectively [33]. The fluid was injected from the borehole after the geostatic step. A line source term is applied to the borehole. One additional layer of elements in the borehole was considered, in which the phase-field $v = 0$, and the initial width is given as the size of the element ($h_e = 0.003$ m). The material parameters for the porous medium and the fluid are listed in Table 1.

We first investigated the initial strain and stress fields after the geostatic step. For the homogeneous model, the different strain decomposition models, i.e., isotropic, volumetric–deviatoric, and no-tension models, gave the same results as shown in Figure 2. The initial strain is zero, and the initial stress is well-distributed.

Table 1. Values of material parameters.

Parameters	Values	Unit
Young's modulus (E_0)	20×10^4	MPa
Poisson's ratio (v_0)	0.2	-
Biot's coefficient (α_m)	0.6	-
Porosity (ϕ_m)	0.02	-
Permeability (k_m)	10^{-16}	m^2
Critical fracture energy release rate ($\mathcal{G}_c$)	200	N/m
Length scale parameter ℓ	0.006	m
Fluid viscosity (μ)	10^{-4}	Pa·s
Fluid compressibility (c_f)	4.55×10^{-10}	Pa^{-1}
Injection rate (Q)	2×10^{-4}	m/s

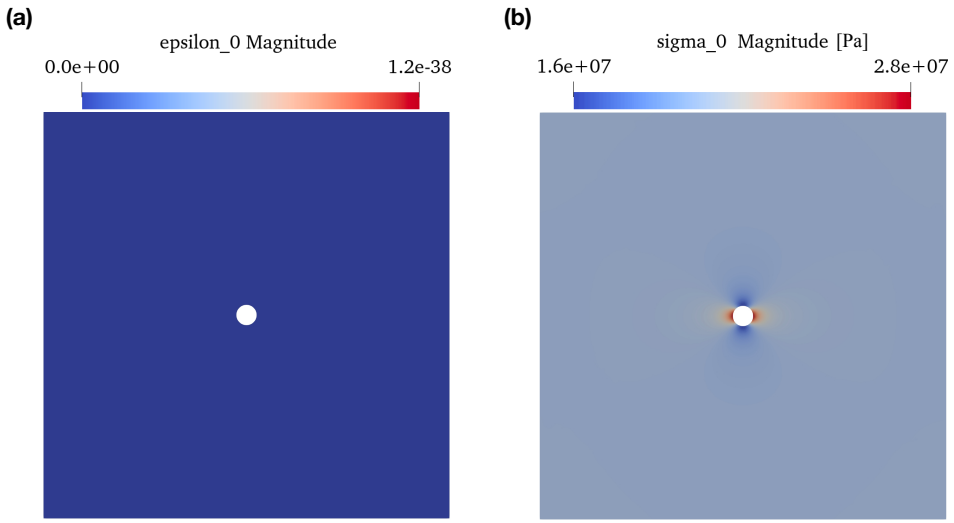


Figure 2. The strain (**a**) and stress (**b**) field after the geostatic step for the homogeneous model with the confining pressures being $\sigma_v = 9.7$ MPa and $\sigma_h = 17.2$ MPa, where the 'epsilon_0' and 'sigma_0' denote the initial strain and stress states from which the simulation (fluid injection) starts.

When the natural fractures were considered, these three strain decomposition models show different results, as shown in Figure 3. For the isotropic model, the fracture domain does not experience stiffness recovery in compression because the full stiffness is degraded by the phase field. The stress is highly concentrated in the crack tip, which is likely to nucleate new cracks if no appropriate geostatic step is considered. Following the proposed two-step strategy, the initial strain is reduced to an acceptable value less than 3.3×10^{-6} so that we do not see phase-field evolution.

For the volumetric–deviatoric and no-tension models, the stress concentration is not that strong. The two-step strategy works well to reach zero initial strain. However, the stress field predicted by the volumetric–deviatoric model still shows some disturbance, revealing an unsatisfactory stiffness recovery behavior when the fracture is compressed. On the other hand, the no-tension model excludes stiffness degradation under any compression state so that it can recover the homogeneous results, as shown in Figures 2 and 3c.

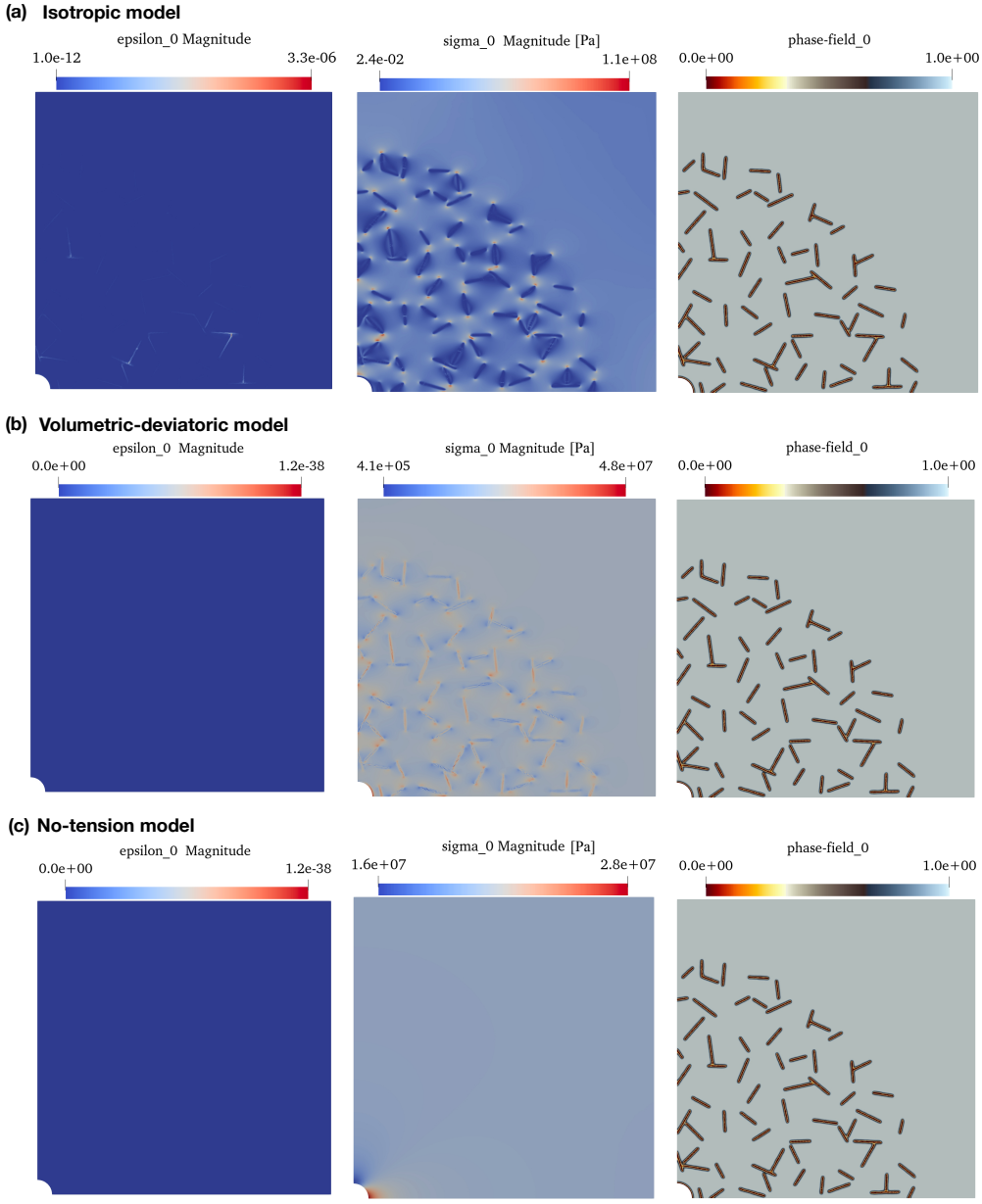


Figure 3. The initial state of the naturally fractured model after the geostatic step for the isotropic model (**a**), volumetric-deviatoric model (**b**) and no-tension model (**c**), with the confining pressures being $\sigma_v = 9.7$ MPa and $\sigma_h = 17.2$ MPa.

3.2. Fracture Propagation from a Borehole

The effect of in situ stress on the nucleation and propagation of hydraulic fractures was then investigated. The isotropic model was used. In Figure 4, the horizontal confining pressure is a major stress, and the hydraulic fracture nucleates and propagates horizontally. The crack initiates at both sides of the borehole and propagates symmetrically at the beginning. This symmetry is broken when the crack propagates for a certain distance, and only the right side of the fracture continues to propagate while the left side stops propagating. The fluid flows along the fracture and decreases when the fracture propagates.

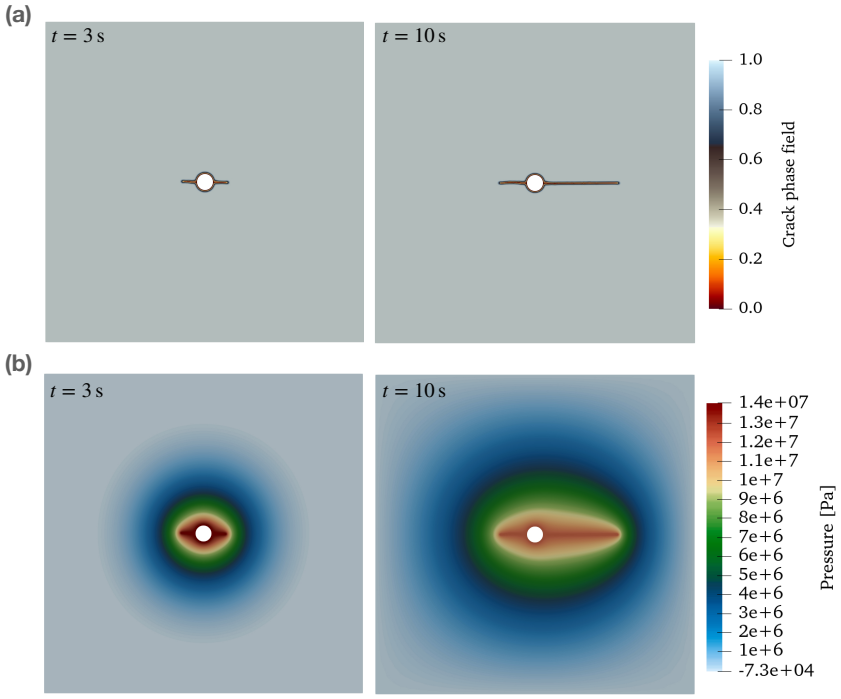


Figure 4. Hydraulic fracture propagation along the horizontal direction (**a**) and the correponding pressure field (**b**), with the confining pressures being $\sigma_v = 9.7$ MPa and $\sigma_h = 17.2$ MPa.

When the vertical confining pressure is the major one, as shown in Figure 5, the hydraulic fracture nucleates and propagates vertically, and it shows the same symmetric and breaking symmetry behaviors. The value of the pressure is in the same range as in Figure 4, except that the distribution becomes vertical.

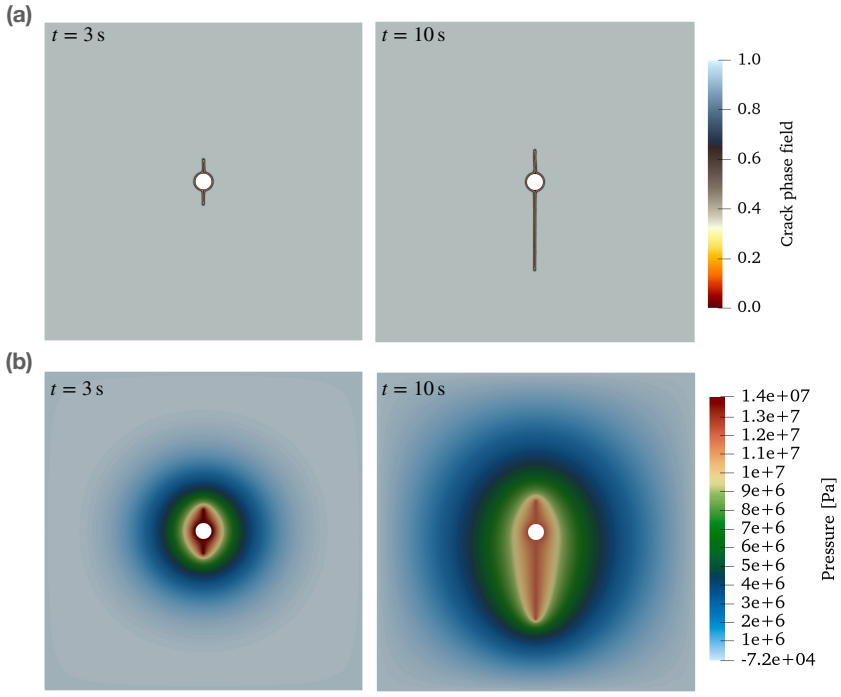


Figure 5. Hydraulic fracture propagation along the vertical direction (**a**) and the corresponding pressure field (**b**), with the confining pressures being $\sigma_v = 17.2$ MPa and $\sigma_h = 9.7$ MPa.

As a short summary, after the geostatic step, we reproduced the propagation of the hydraulic fracture along the direction of the maximum principal stress. Furthermore, since

zero or near-zero initial strain field is ensured, high confining pressures can be considered without worrying about inducing undesired phase-field evolution. This feature is pivotal for extending the application of the phase-field models to deep underground conditions.

3.3. Crack Nucleation and Critical Pressure

We then study the crack nucleation for different strain decomposition schemes under high confining pressure. The crack nucleation problem using the phase-field model has been investigated, for example, in [7,34,35]. However, there has been less study of the nucleation of hydraulic fractures using the phase-field model, especially in a variationally consistent manner. Notably, Fan et al. [36] introduced a stress-based fracture nucleation criterion and showed a good match with the analytical solution by Haimson and Fairhurst [37]. This section numerically investigates crack nucleation for different strain-based models with eigenstrain (equivalent to geostatic stress).

Taking $\sigma_v = 9.7$ MPa and $\sigma_h = 17.2$ MPa as an example, three different strain decomposition schemes are considered in Figure 6. The mesh for these three model remains the same, as shown in Figure 1a. The numerical results show that only horizontal hydraulic fractures were nucleated from the borehole. The volumetric–deviatoric model generates similar hydraulic fracturing nucleation, and the no-tension model leads to a slight change in the location of the crack nucleation compared to the other two models.

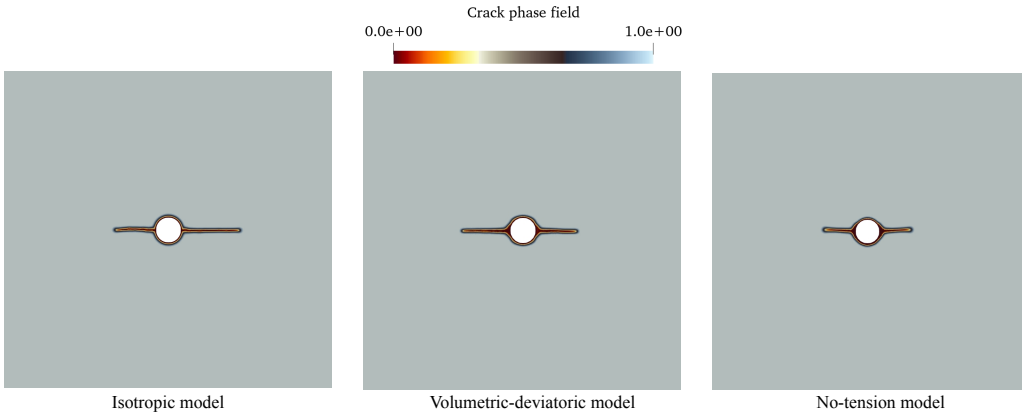


Figure 6. Hydraulic fracture propagation using different strain decomposition models, with the confining pressures being $\sigma_v = 9.7$ MPa and $\sigma_h = 17.2$ MPa.

The critical pressures with and without the geostatic step are compared in Figure 7, in which we reduce the confining pressure $\sigma_v = 0$ Mpa and $\sigma_h = 2$ MPa to avoid phase-field evolution before injection because of stress concentration at the borehole. It can be found that the critical pressure is higher when considering the geostatic step because an eigenstrain is introduced in Equation (20), leading to a smaller value of true strain $\boldsymbol{\varepsilon}$ (contributing to the phase-field evolution) compared with the case without the geostatic step.

The eigenstrain $\boldsymbol{\varepsilon}^*$ in Equation (20) remains unchanged after the geostatic step, and its value will affect the calculation of effective stiffness for strain decomposition models, such as volumetric–deviatoric and no-tension models. When the total strain is updated due to fluid injection, the true strain that drives phase-field evolution will be altered by $\boldsymbol{\varepsilon}^*$, and the location with respect to the crack nucleation criterion will also be changed. This makes crack nucleation more unpredictable. Although the isotropic model seems to yield the expected hydraulic fracturing, it is not safe to conclude its validity, as the stiffness recovery cannot be captured. Therefore, it may cause unrealistic fracture propagation when natural fractures are considered. For the volumetric–deviatoric model, the stiffness is partially recovered when the volumetric strain is less than zero, i.e., compression, whereas the shear fracture can still be activated around the borehole while keeping the fluid injection. Furthermore, the shear strength predicted by the volumetric–deviatoric model is underestimated [25,38]. On the other hand, the no-tension model retains the stiffness recovery under

compression but excludes the shear fracture, which might be a main fracture pattern under high confining pressures.

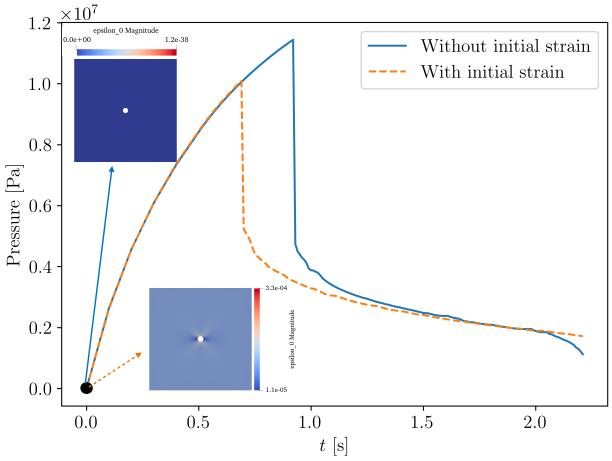


Figure 7. The average pressure on the borehole with and without the geostatic step under the confining pressures $\sigma_v = 0$ MPa and $\sigma_h = 2$ MPa.

3.4. Fracture Propagation Interaction with Natural Fractures

Finally, the hydraulic fracturing in the naturally fractured porous medium was considered. As studied before, the no-tension model gave the most reasonable initial state (Figure 3) and stiffness recovery. We used the no-tension model in this case, and the confining pressures were taken as $\sigma_v = 9.7$ MPa and $\sigma_h = 17.2$ MPa. Figure 8 shows that the hydraulic fracture initiated from the borehole interacted with the natural fracture. Depending on the intersection angle, the hydraulic fracture merges with the natural fracture with a small intersection angle and penetrates the natural fracture with a high intersection angle.

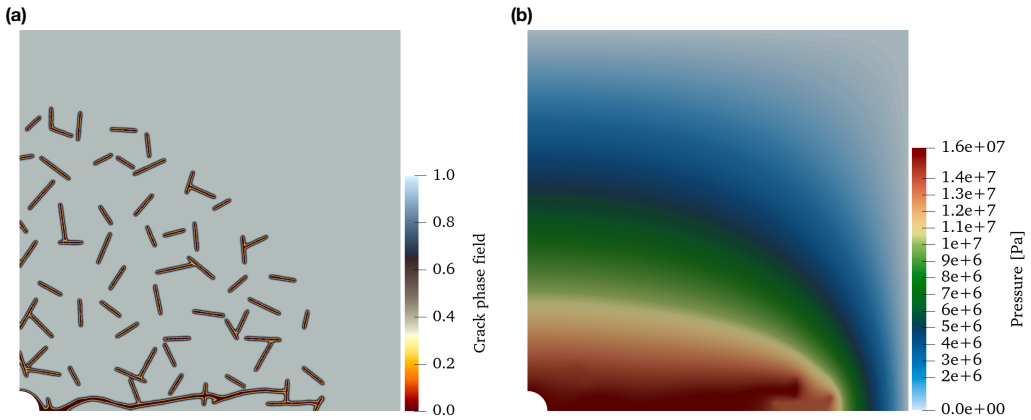


Figure 8. Hydraulic fracture propagation interacted with the natural fractures (**a**) and the corresponding pressure field (**b**) with the confining pressures being $\sigma_v = 9.7$ MPa and $\sigma_h = 17.2$ MPa.

4. Conclusions

This paper studied how in situ stress can be considered without inducing unrealistic crack evolution when different strain decomposition schemes are used in the phase-field modeling of hydraulic fracturing. After presenting a micromechanics-based hydromechanical phase-field model, a two-step strategy was proposed to accommodate geostatic stresses in phase-field modeling, where the geostatic stresses are represented by an eigenstrain. Two numerical examples demonstrated that the proposed two-step strategy can reach a desired initial state, i.e., with geostatic stresses and zero strain, and even complex natural fractures are considered. This two-step strategy is expected to extend phase-field modeling under high confinement when considering deep underground projects. Additionally, commonly used strain decomposition schemes, such as the isotropic and volumetric–deviatoric

models, pose some challenges in capturing stiffness recovery at fracture closure and shear fracture nucleation under high confining pressures. In future work, stress-based fracture nucleation criteria would be a promising alternative.

Funding: This research was funded by the National Natural Science Foundation of China (Grant No. 12202137).

Data Availability Statement: Data are contained within the article.

Acknowledgments: The author is very grateful to the OpenGeoSys developer team for technical advice in coding and software implementation support.

Conflicts of Interest: The author declares no conflicts of interest.

References

1. Olasolo, P.; Juárez, M.; Morales, M.; Liarte, I. Enhanced geothermal systems (EGS): A review. *Renew. Sustain. Energy Rev.* **2016**, *56*, 133–144. [CrossRef]
2. Matos, C.R.; Carneiro, J.F.; Silva, P.P. Overview of large-scale underground energy storage technologies for integration of renewable energies and criteria for reservoir identification. *J. Energy Storage* **2019**, *21*, 241–258. [CrossRef]
3. Shukla, R.; Ranjith, P.; Haque, A.; Choi, X. A review of studies on CO_2 sequestration and caprock integrity. *Fuel* **2010**, *89*, 2651–2664. [CrossRef]
4. Meyer, B.R.; Bazan, L.W. A discrete fracture network model for hydraulically induced fractures-theory, parametric and case studies. In Proceedings of the SPE Hydraulic Fracturing Technology Conference and Exhibition, The Woodlands, TX, USA, 26 January 2011; p. SPE-140514-MS.
5. Lei, Q.; Latham, J.P.; Tsang, C.F. The use of discrete fracture networks for modelling coupled geomechanical and hydrological behaviour of fractured rocks. *Comput. Geotech.* **2017**, *85*, 151–176. [CrossRef]
6. Bourdin, B.; Francfort, G.A.; Marigo, J.J. Numerical experiments in revisited brittle fracture. *J. Mech. Phys. Solids* **2000**, *48*, 797–826. [CrossRef]
7. Tanné, E.; Li, T.; Bourdin, B.; Marigo, J.J.; Maurini, C. Crack nucleation in variational phase-field models of brittle fracture. *J. Mech. Phys. Solids* **2018**, *110*, 80–99. [CrossRef]
8. Wu, J.Y.; Nguyen, V.P.; Nguyen, C.T.; Sutula, D.; Sinaie, S.; Bordas, S.P. Phase-field modeling of fracture. *Adv. Appl. Mech.* **2020**, *53*, 1–183.
9. Borden, M.J.; Verhoosel, C.V.; Scott, M.A.; Hughes, T.J.; Landis, C.M. A phase-field description of dynamic brittle fracture. *Comput. Methods Appl. Mech. Eng.* **2012**, *217*, 77–95. [CrossRef]
10. Miehe, C.; Mauthe, S. Phase field modeling of fracture in multi-physics problems. Part III. Crack driving forces in hydro-poro-elasticity and hydraulic fracturing of fluid-saturated porous media. *Comput. Methods Appl. Mech. Eng.* **2016**, *304*, 619–655. [CrossRef]
11. Wilson, Z.A.; Landis, C.M. Phase-field modeling of hydraulic fracture. *J. Mech. Phys. Solids* **2016**, *96*, 264–290. [CrossRef]
12. Chukwudozie, C.; Bourdin, B.; Yoshioka, K. A variational phase-field model for hydraulic fracturing in porous media. *Comput. Methods Appl. Mech. Eng.* **2019**, *347*, 957–982. [CrossRef]
13. Yi, L.P.; Waisman, H.; Yang, Z.Z.; Li, X.G. A consistent phase field model for hydraulic fracture propagation in poroelastic media. *Comput. Methods Appl. Mech. Eng.* **2020**, *372*, 113396. [CrossRef]
14. Yi, L.P.; Li, X.G.; Yang, Z.Z.; Yang, C.X. Phase field modeling of hydraulic fracturing in porous media formation with natural fracture. *Eng. Fract. Mech.* **2020**, *236*, 107206. [CrossRef]
15. Lepillier, B.; Yoshioka, K.; Parisio, F.; Bakker, R.; Bruhn, D. Variational Phase-field modeling of hydraulic fracture interaction with natural fractures and application to enhanced geothermal systems. *J. Geophys. Res. Solid Earth* **2020**, *125*, e2020JB019856. [CrossRef]
16. Zhuang, X.; Zhou, S.; Sheng, M.; Li, G. On the hydraulic fracturing in naturally-layered porous media using the phase field method. *Eng. Geol.* **2020**, *266*, 105306. [CrossRef]
17. Yoshioka, K.; Mollaali, M.; Kolditz, O. Variational phase-field fracture modeling with interfaces. *Comput. Methods Appl. Mech. Eng.* **2021**, *384*, 113951. [CrossRef]
18. Warpinski, N.R.; Schmidt, R.A.; Northrop, D.A. In-situ stresses: The predominant influence on hydraulic fracture containment. *J. Pet. Technol.* **1982**, *34*, 653–664. [CrossRef]
19. Zhang, Y.; Zhang, J.; Yuan, B.; Yin, S. In-situ stresses controlling hydraulic fracture propagation and fracture breakdown pressure. *J. Pet. Sci. Eng.* **2018**, *164*, 164–173. [CrossRef]
20. Hubbert, M.K.; Willis, D.G. Mechanics of hydraulic fracturing. *Trans. AIME* **1957**, *210*, 153–168. [CrossRef]
21. Zhou, S.; Zhuang, X.; Rabczuk, T. Phase field method for quasi-static hydro-fracture in porous media under stress boundary condition considering the effect of initial stress field. *Theor. Appl. Fract. Mech.* **2020**, *107*, 102523. [CrossRef]
22. Salvati, E. Residual stress as a fracture toughening mechanism: A Phase-Field study on a brittle material. *Theor. Appl. Fract. Mech.* **2021**, *114*, 103021. [CrossRef]

23. Zhang, C.; Zhang, J.; Li, H.; Li, Y.; Xu, W.; Qiang, S.; Yuan, M. A phase field approach to the fracture simulation of quasi-brittle structures with initial state. *Eng. Fract. Mech.* **2024**, *304*, 110150. [CrossRef]
24. You, T.; Yoshioka, K. On poroelastic strain energy degradation in the variational phase-field models for hydraulic fracture. *Comput. Methods Appl. Mech. Eng.* **2023**, *416*, 116305. [CrossRef]
25. Amor, H.; Marigo, J.J.; Maurini, C. Regularized formulation of the variational brittle fracture with unilateral contact: Numerical experiments. *J. Mech. Phys. Solids* **2009**, *57*, 1209–1229. [CrossRef]
26. Freddi, F.; Royer-Carfagni, G. Regularized variational theories of fracture: A unified approach. *J. Mech. Phys. Solids* **2010**, *58*, 1154–1174. [CrossRef]
27. Pham, K.; Amor, H.; Marigo, J.J.; Maurini, C. Gradient damage models and their use to approximate brittle fracture. *Int. J. Damage Mech.* **2011**, *20*, 618–652. [CrossRef]
28. Bunger, A.P.; Detournay, E.; Garagash, D.I. Toughness-dominated hydraulic fracture with leak-off. *Int. J. Fract.* **2005**, *134*, 175–190. [CrossRef]
29. Lee, S.; Wheeler, M.F.; Wick, T. Iterative coupling of flow, geomechanics and adaptive phase-field fracture including level-set crack width approaches. *J. Comput. Appl. Math.* **2017**, *314*, 40–60. [CrossRef]
30. Xu, Y.; You, T.; Zhu, Q. Reconstruct lower-dimensional crack paths from phase-field point cloud. *Int. J. Numer. Methods Eng.* **2023**, *124*, 3329–3351. [CrossRef]
31. Naumov, D.; Bilke, L.; Lehmann, C.; Fischer, T.; Wang, W.; Silbermann, C.; Thiedau, J.; Selzer, P. OpenGeoSys 2024. Available online: https://zenodo.org/records/11652195 (accessed on 14 July 2024).
32. Kim, J.; Tchelepi, H.A.; Juanes, R. Stability and convergence of sequential methods for coupled flow and geomechanics: Fixed-stress and fixed-strain splits. *Comput. Methods Appl. Mech. Eng.* **2011**, *200*, 1591–1606. [CrossRef]
33. He, Q.; Zhu, L.; Li, Y.; Li, D.; Zhang, B. Simulating hydraulic fracture re-orientation in heterogeneous rocks with an improved discrete element method. *Rock Mech. Rock Eng.* **2021**, *54*, 2859–2879. [CrossRef]
34. Kumar, A.; Bourdin, B.; Francfort, G.A.; Lopez-Pamies, O. Revisiting nucleation in the phase-field approach to brittle fracture. *J. Mech. Phys. Solids* **2020**, *142*, 104027. [CrossRef]
35. De Lorenzis, L.; Maurini, C. Nucleation under multi-axial loading in variational phase-field models of brittle fracture. *Int. J. Fract.* **2022**, *237*, 61–81. [CrossRef]
36. Fei, F.; Costa, A.; Dolbow, J.E.; Settgast, R.R.; Cusini, M. A phase-field model for hydraulic fracture nucleation and propagation in porous media. *Int. J. Numer. Anal. Methods Geomech.* **2023**, *47*, 3065–3089. [CrossRef]
37. Haimson, B.; Fairhurst, C. Initiation and extension of hydraulic fractures in rocks. *Soc. Pet. Eng. J.* **1967**, *7*, 310–318. [CrossRef]
38. Vicentini, F.; Zolesi, C.; Carrara, P.; Maurini, C.; De Lorenzis, L. On the energy decomposition in variational phase-field models for brittle fracture under multi-axial stress states. *Int. J. Fract.* **2024**, 1–27. [CrossRef]

Disclaimer/Publisher's Note: The statements, opinions and data contained in all publications are solely those of the individual author(s) and contributor(s) and not of MDPI and/or the editor(s). MDPI and/or the editor(s) disclaim responsibility for any injury to people or property resulting from any ideas, methods, instructions or products referred to in the content.